Future Science Prospects for AMI

Keith Grainge,[1,2] Paul Alexander,[1,2] Richard Battye,[3] Mark Birkinshaw,[4] Andrew Blain,[5] Malcolm Bremer,[4] Sarah Bridle,[6] Michael Brown,[3] Richard Davis,[3] Clive Dickinson,[3] Alastair Edge,[7] George Efstathiou,[2] Robert Fender,[8] Martin Hardcastle,[9] Jennifer Hatchell,[10] Michael Hobson,[1] Matthew Jarvis,[11,12] Benjamin Maughan,[4] Ian McHardy,[8] Matthew Middleton,[7] Anthony Lasenby,[1,2] Richard Saunders,[1,2] Giorgio Savini,[13] Anna Scaife,[8] Graham Smith,[14] Mark Thompson,[9] Glenn White,[15,16] Kris Zarb-Adami,[11,17] James Allison,[18] Jane Buckle,[1] Alberto Castro-Tirado,[19] Maria Chernyakova,[20] Roger Deane,[21] Farhan Feroz,[1] Ricardo Génova-Santos,[22] David Green,[1] Diana Hannikainen,[23,24] Ian Heywood,[11] Natasha Hurley-Walker,[25] Rüdiger Kneissl,[26,27] Karri Koljonen,[24] Shrinivas Kulkarni,[28] Sera Markoff,[29] Carrie MacTavish,[2] Michael McCollough,[30] Simone Migliari,[31] Jon M. Miller,[32] James Miller-Jones,[25] Malak Olamaie,[1] Zsolt Paragi,[33] Timothy Pearson,[34] Guy Pooley,[1] Katja Pottschmidt,[35] Rafael Rebolo,[22] John Richer,[1] Julia Riley,[1] Jérôme Rodriguez,[36] Carmen Rodríguez-Gonzálvez,[37] Anthony Rushton,[38] Petri Savolainen,[24] Paul Scott,[1] Timothy Shimwell,[39] Marco Tavani,[40] John Tomsick,[41] Valeriu Tudose,[42] Kurt van der Heyden,[21] Alexander van der Horst,[43] Angelo Varlotta,[44] Elizabeth Waldram,[1] Joern Wilms,[45] Andrzej Zdziarski,[46] Jonathan Zwart,[12] Yvette Perrott,[1] Clare Rumsey,[1] and Michel Schammel[1]

[1] *Astrophysics Group, Cavendish Laboratory, J J Thomson Avenue, Cambridge, CB3 0HE UK*
[2] *Kavli Institute for Cosmology Cambridge, Madingley Road, Cambridge CB3 0HA, UK*
[3] *Alan Turing Building, School of Physics and Astronomy, Oxford Road, Manchester M13 9PL, UK*
[4] *HH Wills Physics Laboratory, University of Bristol, Tyndall Avenue, Bristol BS8 1TL, UK*
[5] *Department of Physics and Astronomy, University of Leicester, LE1 7RH Leicester, UK*
[6] *Department of Physics & Astronomy, University College London, Gower Street, London WC1E 6BT, UK*
[7] *Department of Physics, University of Durham, South Road, Durham DH1 3LE, UK*
[8] *Physics and Astronomy, University of Southampton, Southampton SO17 1BJ, UK*
[9] *Centre for Astrophysics Research, Science & Technology Research Institute, University of Hertfordshire, Hatfield, UK*
[10] *School of Physics, University of Exeter, Stocker Road, Exeter EX4 4QL*
[11] *Astrophysics, Department of Physics, University of Oxford, Keble Road, Oxford OX1 3RH, UK*
[12] *Physics Department, University of the Western Cape, Bellville 7535, South Africa*
[13] *Optical Science Laboratory, University College London, Gower Street, London, UK*
[14] *School of Physics and Astronomy, University of Birmingham, Edgbaston, Birmingham, B15 2TT, UK*
[15] *RAL Space, STFC Rutherford Appleton Laboratory, Chilton, Didcot, Oxfordshire, OX11 0QX, UK*
[16] *Department of Physics and Astronomy, The Open University, Walton Hall, Milton Keynes, MK7 6AA, UK*
[17] *Department of Physics, Faculty of Science, University of Malta, Malta*
[18] *Sydney Institute for Astronomy, School of Physics A28, University of Sydney, NSW 2006, Australia*
[19] *Instituto de Astrofísica de Andalucia (IAA-CSIC), Glorieta de la Astronomia s/n, 18.008 Granada, Spain*
[20] *Dublin City University, Dublin 9, Ireland; Dublin Institute for Advanced Studies, 31 Fitzwilliam Place, Dublin 2, Ireland*
[21] *Astrophysics, Cosmology and Gravitation Centre, University of Cape Town, Rondebosch 7701, Cape Town, South Africa*
[22] *Instituto de Astrofísica de Canarias,Vía Láctea, 38205 La Laguna, Tenerife, Spain*
[23] *Department of Physics and Space Sciences, Florida Institute of Technology, 150 W. University Blvd., Melbourne, FL, USA*
[24] *Aalto University Metsähovi Radio Observatory, Metsahovintie 114, FIN-02540 Kylmala, Finland*
[25] *International Centre for Radio Astronomy Research - Curtin University, GPO Box U1987, Perth, WA 6845, Australia*
[26] *European Southern Observatory, ESO Vitacura, Alonso de Cordova 3107, Vitacura, Casilla 19001, Santiago, Chile*
[27] *ALMA Santiago Central Offices, Alonso de Cordova 3107, Vitacura, Casilla 7630355, Santiago, Chile*
[28] *Division of Physics, Mathematics and Astronomy, California Institute of Technology, Pasadena, CA 91125, USA*
[29] *Astronomical Institute Anton Pannekoeka, University of Amsterdam, Postbus 94249, 1090 GE Amsterdam, the Netherlands*
[30] *Smithsonian Astrophysical Observatory, 60 Garden Street, Cambridge, MA 02138-1516, USA*
[31] *Departament d'Astronomia i Meteorologia, Universitat de Barcelona, Marti Franqus 1, 08028 Barcelona, Spain*
[32] *Department of Astronomy, University of Michigan, 500 Church St, Ann Arbor, MI 48109-1042, USA*
[33] *Joint Institute for VLBI in Europe (JIVE), Postbus 2, 7990 AA Dwingeloo, The Netherlands*
[34] *Cahill Center for Astronomy and Astrophysics, California Institute of Technology, Pasadena, CA 91125, USA*
[35] *CRESST and NASA Goddard Space Flight Center, Code 661, Greenbelt, MD 20771,USA*
[36] *Laboratoire AIM, CEA/IRFU - Universite Paris Diderot, CEA DSM/IRFU/SAp, F-91191 Gif-sur-Yvette, France*
[37] *Spitzer Science Center, MS 220-6, California Institute of Technology, Pasadena, CA 91125 USA*
[38] *European Southern Observatory Karl-Schwarzschild-Str 2, 85748 Garching, Germany*
[39] *CSIRO Astronomy & Space Science, Australia Telescope National Facility, PO Box 76, Epping, NSW 1710, Australia*
[40] *INAF/IASF-Roma, I-00133 Roma, Italy*
[41] *Space Sciences Laboratory, 7 Gauss Way, University of California, Berkeley, CA 94720-7450, USA*
[42] *Institute for Space Sciences, Bucharest, Romania*
[43] *Astronomical Institute Anton Pannekoek, University of Amsterdam, Science Park 904, 1098XH Amsterdam, The Netherlands*
[44] *Purdue University, West Lafayette, IN 47907, USA*
[45] *Dr Karl-Remeis-Sternwarte and Erlangen Center for Astroparticle Physics, Sternwartstr. 7, 96049 Bamberg, Germany*
[46] *Nicolaus Copernicus Astronomical Center, ul. Bartycka 18, 00-716 Warsaw, Poland*

Abstract

The Arcminute Microkelvin Imager (AMI) [23] is a telescope specifically designed for high sensitivity measurements of low-surface-brightness features at cm-wavelength and has unique, important capabilities. It consists of two interferometer arrays operating over 13.5–18 GHz that image structures on scales of 0.5–10 arcmin with very low systematics. The Small Array (AMI-SA; ten 3.7-m antennas) couples very well to Sunyaev-Zel'dovich (SZ) features from galaxy clusters and to many Galactic features. The Large Array (AMI-LA; eight 13-m antennas) has a collecting area ten times that of the AMI-SA and longer baselines, crucially allowing the removal of the effects of confusing radio point sources from regions of low surface-brightness, extended emission. Moreover AMI provides fast, deep object surveying and allows monitoring of large numbers of objects. In this White Paper we review the new science — both Galactic and extragalactic — already achieved with AMI and outline the prospects for much more.

Contents

I. SUNYAEV-ZEL'DOVICH EFFECT FROM GALAXY CLUSTERS

A. Introduction

Clusters of galaxies are the most massive bound structures in the cosmic web of large-scale structure. They evolve through the linear regime from the density perturbations imaged in the primordial cosmic microwave background (CMB) and then continue to grow in the non-linear regime through in-fall and mergers. As such, clusters have great potential for use in cosmology, both to investigate the aspects of the underlying cosmological model (e.g. σ_8) and as cosmographic buoys to study the evolution of structure as a whole in the universe (see e.g. Allen, Evrard, & Mantz [3]). In order to connect clusters to the underlying cosmology, the critical parameter that must be measured is their mass. Various scaling relations have been proposed for mass determination, but the Comptonisation Y parameter is now recognised as a highly-reliable mass indicator [66]. This is, of course, measured directly through SZ measurements, without the need for a model-dependent calculation from the data as is the case for X-rays. The redshift-independence of SZ surface brightness offers the possibility of observing clusters right back to their epoch of formation; and the linear (as opposed to quadratic) dependence of the SZ signal on gas density allows imaging of the outer regions of the Intra Cluster Medium (ICM) — Allen, Evrard, & Mantz [3] emphasise the importance of investigating these outer regions, which is challenging in X-rays, but straightforward in SZ. Combining SZ measurements with X-ray observations and optical-lensing data gives essential, new information.

In addition to their use for cosmology, clusters are of fundamental interest in their own right, harbouring a great deal of detailed ICM astrophysics (see e.g. Kunz et al. [69]). For example, merger events are laboratories in which the nature of dark matter can be tested [39]. Imaging of detailed ICM structure is now becoming possible in both X-ray and SZ (e.g. Korngut et al. [65], Mason et al. [74]), allowing measurement of density and temperature over a range of scales. A critical issue in understanding the ICM is the role of magnetic field. This could substantially stiffen the ICM equation of state, affect cluster dynamics and evolution, and lead to bias in many mass estimations. Little is known about ICM magnetic field, because the requisite measurements have been out of reach: however, the instrumental situation is now changing.

The initial science drivers for AMI were, via Sunyaev-Zel'dovich effect (SZ) measurements, to constrain cosmology through conducting a blind survey for galaxy clusters; and to explore the physics of clusters and tie down their scaling relations and evolution through pointed observations towards known or candidate clusters. AMI has made significant advances in both of these areas.

B. Blind cluster SZ surveys

We have surveyed 10 first-look fields to target sensitivities of 100 μJy and 60 μJy with AMI's Small (SA) and Large (LA) arrays respectively. Each candidate cluster identified through this analysis is then reobserved with deep, pointed observations to verify the detection. In AMI Consortium: Shimwell et al. [22] we describe the first successful cluster detection from the first (blind) field to be completed (see Figure 1). This distant, remarkably extended system, probably a merger, is detected at very high significance by AMI in SZ. We calculate that the cluster mass limit to which our survey will be sensitive as $2 \times 10^{14} M_{\odot}$ by scaling from the reported detection.

A full Bayesian analysis [10] of the first 10 fields is underway to detect clusters, determine their significance and place constraints on cosmological parameters, e.g. σ_8. In addition, the AMI-LA observations of our fields have allowed us to measure the radio source counts at 15.7 GHz down to 0.5 mJy [6, 7]; this 10C survey is the deepest radio survey of any significant extent above 1.4 GHz. New programme of observations will push the source counts a further factor of three deeper. Preliminary results suggest the detection of a change in the slope of the source counts and a change in the spectral index distribution, both of which indicate a change in the radio source population.

AMI SZ-surveying and analysis is now routine and has been demonstrated to detect clusters down to a limiting mass of $2 \times 10^{14} M_{\odot}$. Therefore there is a great deal of scientific potential in performing complementary surveys towards fields observed in other wavebands. For example, the AMI blind surveys have now been extended to include additional fields toward the Lockmann Hole and ELAIS N1 regions which have been surveyed deeply by UKIDSS. This ongoing project will allow cross-calibration of IR and SZ scaling relationships and investigation of cluster selection functions of the two methods. This project will also provide a legacy survey of these well-studied regions. Another example of a future collaboration is with Battye et al. on the SuperCLASS legacy programme (http://www.e-merlin.ac.uk/legacy/projects/superclass.html), which has recently been allocated 862 hours of eMERLIN observing time. The aim of this programme is to measure weak gravitation lensing through radio imaging towards a supercluster field. Combining these data with SZ measurements from AMI will set very powerful joint constraints on parameters of baryonic and dark matter structures in this field.

C. Pointed SZ observations

AMI has been used for a wide range of SZ projects targeting fields of interest revealed in other wavebands [5, 8, 11, 12, 24]. We have demonstrated the capabilities of AMI through observations of a variety of different known clusters [24]. We have also used these observations to validate our fully Bayesian analysis tool, McAdam [50], which uses nested sampling to fit various cluster parameterisations efficiently to our data, in particular generating a robust estimate of the key observable of cluster mass out to the virial radius.

AMI has been used for a variety of different pointed SZ programmes: to study the astrophysics of individual clusters of particular interest e.g. the bullet-like cluster Abell 2146 (see Figure 2) and the Corona Borealis supercluster; to produce joint constraints on cluster models once combined with optical lensing data [9]; for statistical analyses of scaling relations through observations towards well-defined samples of clusters drawn from X-ray surveys (e.g. the LOCUSS, BCS and MACS samples). We now detail one particular example as follows.

AMI observations of an X-ray luminosity-limited subset of 19 LoCuSS clusters (which have $0.142 \leq z \leq 0.295$ to minimise cosmic evolution) have yielded 16 SZ detections with significances (of the peaks alone) between 5σ and 23σ (see Figure 3 for SZ maps overlaid on X-ray for four of these clusters). The SZ images span scales out to the cluster virial radii (which very few X-ray images do), and show a larger range of morphology than that seen in published ACT, SPT or CARMA/SZA images (which tend not to reach $r_{\rm virial}$) or in Planck images (which do not have enough angular resolution). Under reasonable assumptions, the cluster plasma temperature can be derived from AMI data alone AMI Consortium: Rodríguez-Gonzálvez C. et al. [12] — unlike the traditional method, no X-ray information is required. In the 10 cases where deep *Chandra* or Suzaku images are available, allowing X-ray temperatures to be measured out to around $0.5 r_{\rm virial}$ (rather than the more common 0.1–$0.2 r_{\rm virial}$), it is clear that there is decent correspondence between these $T_{X,0.5{\rm virial}}$-values and the $T_{AMI,0.5-1{\rm virial}}$ values from SZ, but with some strong outliers that have high $T_{\rm X}$ compared with $T_{\rm AMI}$. These outliers are the strong mergers. AMI easily probes the outer parts of clusters where most of the baryons and dark matter exist; these parts are hard for X-ray instruments to detect even at moderate z. At moderate z, the combination of AMI and *Chandra*/Suzaku is thus very powerful for understanding how clusters work.

There are several ongoing collaborations that will allow joint analysis of our AMI images with data from other wavebands, as summarised below.

- **MACS sample** This is a high-redshift sample and so offers the possibility of investigating potential evolution in cluster properties. Deep *Chandra* data and X-ray temperatures can be used to constrain the priors for our

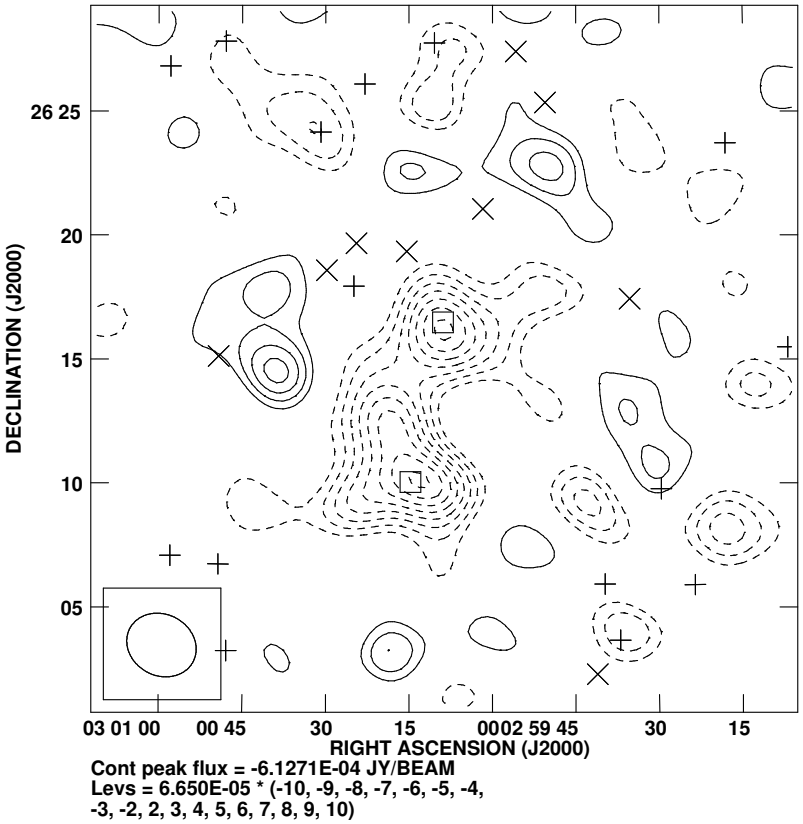

FIG. 1: Map of the SZ effect in the first cluster system to be discovered in the AMI blind survey. positive contours are solid and negative ones dashed; contour levels are in units of σ. Crosses (vertical and diagonal) indicate the position of point radio sources that have been subtracted from the data. Squares show the best fit positions for the clusters. The synthesised beam is indicated in the lower-left corner.

McAdam analysis.

- **The Canadian Cluster Comparison Project (CCCP) sample**. The CCCP team have CFHT lensing observations towards a large sample of X-ray selected clusters; many have been observed with *Chandra* and *XMM*.
- **The CLASH sample**. The CLASH team has lensing data from *HST* and Subaru of a sample of dynamically-relaxed, massive clusters and this will allow us to derive stringent constraints on dark matter and hot baryons in the representative clusters.
- **Serendipitous *XMM* cluster detections** *XMM* images and temperatures will be available for combination with the AMI data.

There continue to be huge opportunities for new science from pointed AMI SZ observations as new cluster samples become available and for joint analyses with other data sets to explore the physics of the intracluster gas of particular systems. In addition, there are possibilities for entirely new AMI SZ science areas, such as attempts to detect the SZ effect from the plasma in filaments of the cosmic web, and combination of a AMI-derived gas model with rotation-measure observations from the new generation of radio observatories such as JVLA and MeerKAT to measure cluster magnetic fields. One of the most exciting opportunities in the short term is support of the *Planck* satellite, which is now providing the first all-sky SZ cluster survey. This is discussed in the section II.

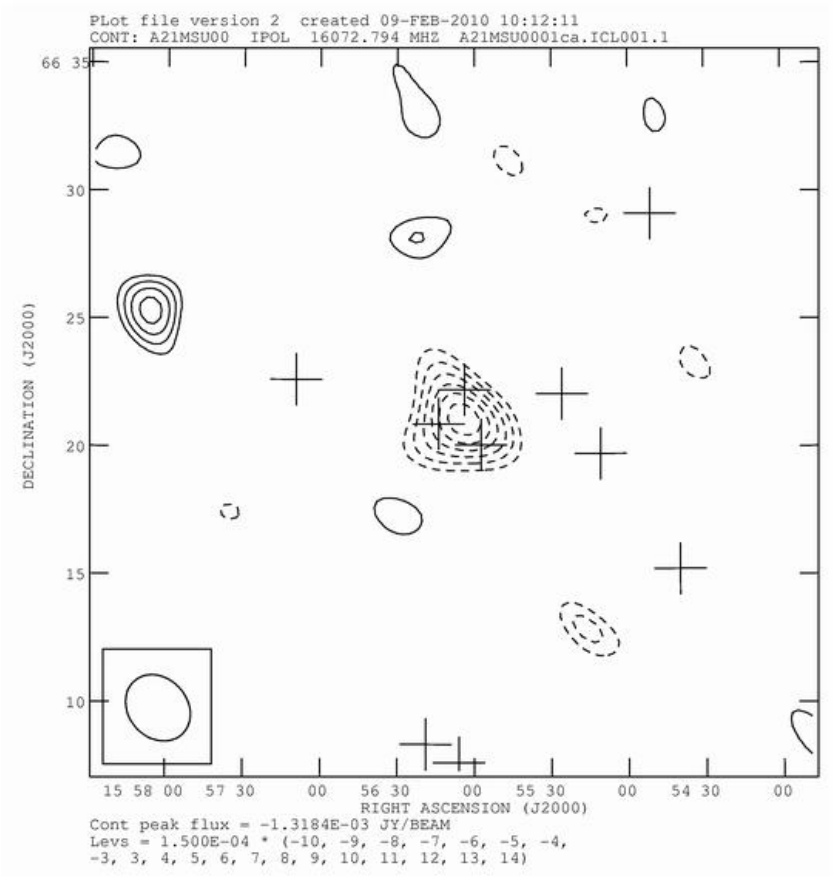

FIG. 2: AMI map of the SZ effect in the Bullet-like cluster A2146. Crosses indicate the positions of subtracted radio sources. The ellipse lower-left indicated the synthesised beam.

D. Comparison of AMI to other SZ telescopes

The South Pole Telescope (SPT) and the Atacama Cosmology Telescope (ACT) are multipixel bolometric telescopes specifically designed for SZ work. They are primarily survey instruments and have already produced extremely exciting results (see e.g. Reichardt et al. [85] for SPT and Marriage et al. [73] for ACT). Both SPT and ACT are conducting very wide field, relatively shallow surveys and so are detecting the rare, most massive clusters in the Universe, while AMI's survey strategy is to spend longer integration times on a smaller area and so sample typical clusters. AMI is therefore able to probe the cluster mass function significantly deeper and so the three telescopes produce useful complementary information on structure formation. AMI is an excellent instrument for pointed follow-up observations on samples of galaxy clusters from other instruments since its 20 arcmin field-of-view matches the typical size of $z > 0.15$ clusters very well; SPT and ACT's very wide fields-of-view mean that their strength is in survey observations. Finally, both ACT and SPT are located in the southern hemisphere with the result that they have little or no (respectively) coverage of the northern sky visible to AMI.

The SZA is now part of the CARMA telescope and so is no longer a dedicated SZ instrument. It is similar in many ways to AMI, but AMI has two key differences which are important for SZ science:

- AMI has access to a factor of two times shorter baselines (in terms of wavelength, i.e. in the uv-plane), and so samples structure out to 10 arcmin, allowing mapping of the gas out to the virial radius in galaxy clusters between z=0.15-2.
- The AMI-LA has ten times the collecting area (and so ten times the flux sensitivity) of the AMI-SA and a good coverage of the uv-plane. This gives very high sensitivity, high image fidelity mapping of the radio point sources, which are the key contaminant and dominant systematic for SZ work. For comparison, SZA configures two of its eight antennas as outriggers for source subtraction, giving comparatively poor flux sensitivity and a single narrow strip of coverage in the uv-plane, resulting in a poor point-spread function and so poor image fidelity.

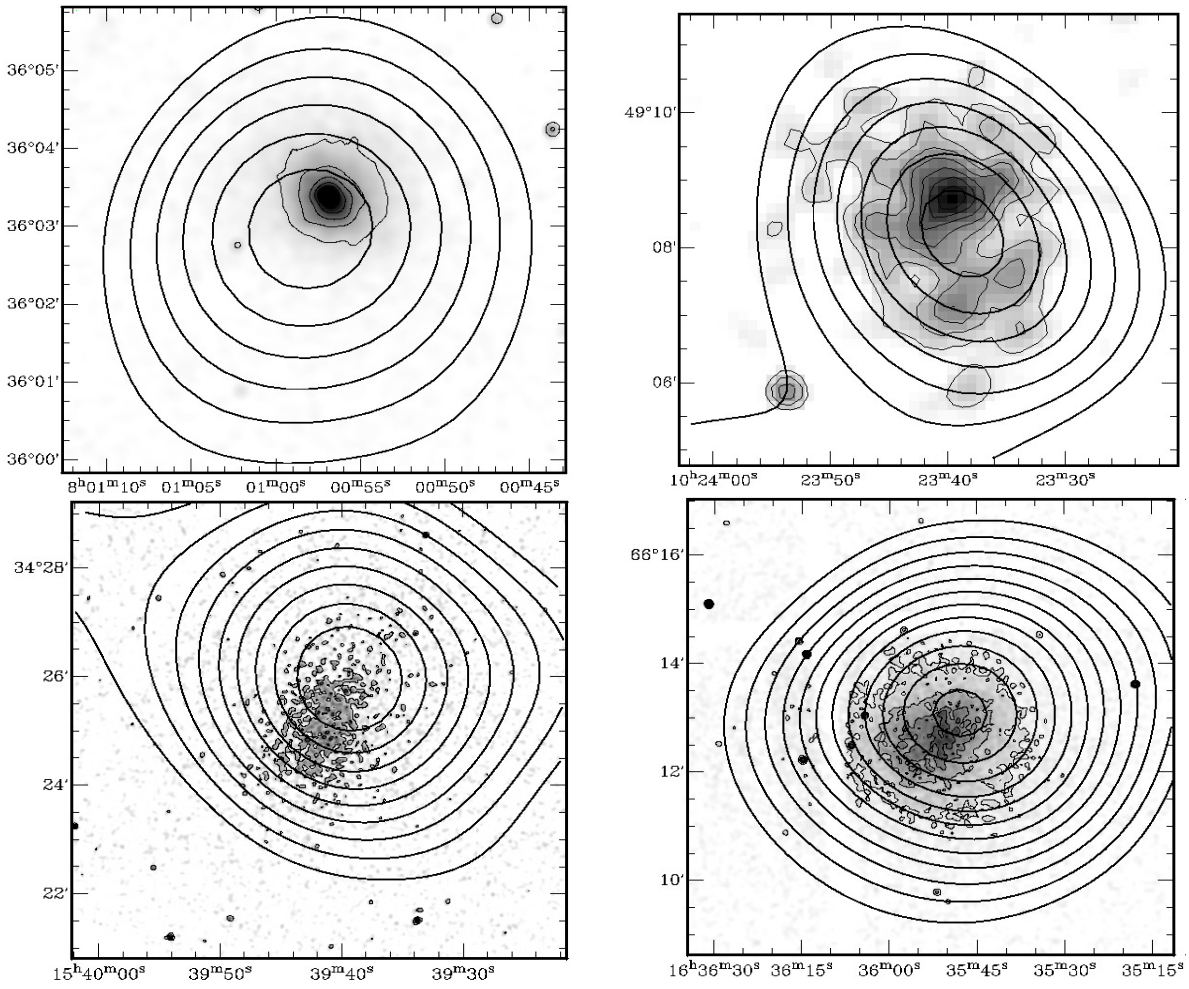

FIG. 3: Maps of four clusters from the LoCuSS sample; from top left: A611, A990, A2111, A2218. Contours show the SZ decrement measured by the AMI-SA after source subtraction, while the greyscale is the X-ray image smoothed *Chandra* data except for A990 which is *ROSAT* HRI).

II. AMI'S ROLE IN *PLANCK* VALIDATION AND FOLLOW-UP

A. Introduction

AMI is very useful for *Planck*-related work in two main contexts — validation and follow-up. Due to restrictions on reporting of *Planck* results before publication, full details of this work will become available early in 2013. However, an MoU between *Planck* and AMI exists covering both these areas, and a broad description of the type of work involved will now be given.

B. Scientific Context

Last year saw the first release of *Planck* results for the SZ effect in clusters of galaxies. The resolution of *Planck* for SZ studies (at best $\simeq 5'$) is lower than for most ground-based observations, but is compensated for by all-sky coverage, plus a good frequency discrimination of the effect due to multiple frequency channels spanning the whole range over which it is important. The 'Early Release SZ Catalogue' (ESZ) [81] contained a sample of 189 clusters of which 169 were previously known. Ground-based telescopes have now confirmed the SZ detections for some of the cluster candidates; AMI provided confirmation within the ESZ paper itself for a previously unknown cluster (see Fig. 4), and has subsequently done the same for a further cluster [8], as well as providing refined position estimates.

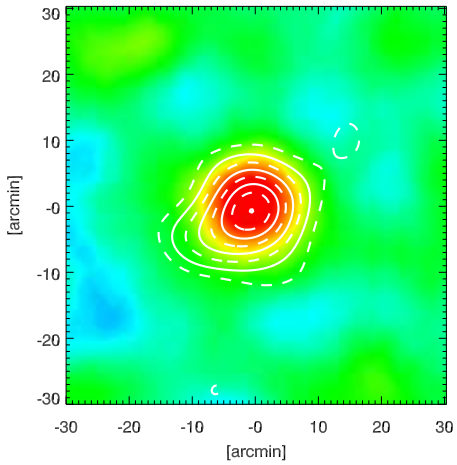

FIG. 4: y-map of PLCKESZ G139.59+24.19 as observed by *Planck* (colour image) and AMI (contours) at a common resolution of 13 arcmin. The contours are from two to nine in S/N ratio. (Taken from Planck Collaboration: Ade et al. [79].)

There is great cosmological interest in the factor of between 0.5 and 0.7 by which the SZ decrements measured by *WMAP7* were lower than what was expected for the given clusters using standard X-ray models for temperature and profile [63]. Some support for a deficit by this same factor came from South Pole Telescope measurements of the SZ power spectrum at high ℓ [72]. However, one of the first *Planck* analyses [81] has found no evidence for a deficit in SZ signal strength in *Planck* data relative to expectations from the X-ray properties of clusters, in apparent contradiction with the *WMAP* results, and highlighting the need to be able to incorporate independent high-resolution SZ data. In Planck Collaboration: Aghanim et al. [81], in addition to emphasising that no deficit has been found, it is pointed out that, even when the analysis is redone in two bins with pressure profiles corresponding to 'cool cores' or 'morphologically disturbed' types, the results are still robust to this, with maximum deviations at only the few percent level. Since this division was thought to be important in explanation of the *WMAP7* results [63], it is unclear currently why there is the apparent discrepancy in findings, though a linkage with assumed profile shape still seems likely. More generally, the comparison of SZ radial profiles with X-ray profiles is an important part of the study of clusters, particularly for the outer regions where AMI excels.

C. AMI Role in Validation and Follow-up

An advantage of SZ verification of candidate clusters discovered in an all-sky satellite survey, is that SZ surface brightness is independent of redshift. This means that even for a high-redshift cluster in which IR, optical or X-ray verification may fail, direct SZ verification is still possible. Detections of this kind, of a candidate high-redshift cluster, are potentially some of the most exciting individual objects that *Planck* will detect, and thus need a high level of reliability associated with them. AMI has the sensitivity to be able to confirm such a detection on a timescale that can make it useful during the verification cycles. Additionally, by performing checks of the SZ levels over a statistically selected sub-sample of all *Planck* SZ detections, a check can be made of the photometric accuracy of the *Planck* SZ amplitude. AMI is also able to provide smaller positional uncertainties on candidates than *Planck* alone, and this feature is also useful in the process of cluster follow-up and validation with optical and X-ray telescopes.

Validation observations can be interleaved with a programme of deeper observations ($\simeq 32\,$hr/cluster) on selected clusters. For rich clusters this will give well resolved $\simeq 20\,\sigma$ detections, including the outer regions of the cluster gas, and provide radio spectra in the 13.5–18.0 GHz range in six spectral channels (which may be useful for constraining the level of possible cluster synchrotron halo emission in combination with data from LOFAR and KAT7). AMI-LA point-source subtraction is able to keep up with the demands of the AMI-SA SZ observations in real time, so these integration times include the time needed to identify and remove contaminating point sources.

The AMI/*Planck* teams have worked on a pilot study involving detailed comparison between SZ measurements obtained by both *Planck* and AMI for a first sample comprising 11 clusters [82]. This involved detailed numerical simulation of the respective responses of the two instruments to a common cluster profile. Since *Planck* and AMI are sensitive to different scales, their comparison and/or combination is already revealing interesting new cluster physics. For example, is the "Universal pressure profile", commonly adopted to describe galaxy clusters [28], sufficient to explain simultaneously the *Planck* and AMI measurements or is there more complicated physics at play? Additionally, the

different sensitivities of Planck and AMI to different regions of scale space, mean it is possible to investigate the potential to break parameter degeneracies, e.g. in the $Y_{SZ} - \theta$ plane, even in an SZ-only analysis. The results of the analysis show an overall broad agreement between the AMI and Planck results but with a tendency for the AMI fluxes to be smaller, suggestive indeed of a possible mismatch in the assumptions about cluster profile.

AMI has continued to play a significant role in Planck cluster validation for a much larger sample of potential new clusters, and extension of the comparison between the Planck and AMI results to the entire sample of clusters visible to AMI in the forthcoming Planck catalogue is currently underway. Ultimately, constraints from other cluster probes (e.g. weak lensing and X-ray measurements) can then also be investigated — in principle the independent constraints within the parameter likelihood planes taking different pairs of methods, should all be consistent, thus providing a stringent test of whether the cluster model and observations are all correct.

III. GALACTIC RESEARCH WITH AMI

A. Introduction

The microwave band is a highly under-utilised spectral window for Galactic research. Historically this is because the expected emission has relatively low surface brightness compared to the longer-wavelength non-thermal Galactic emission and the shorter-wavelength sub-mm and infra-red blackbody emission from thermal dust; emission in the microwave band is predominantly due to the thermal bremsstrahlung, or free-free, mechanism. However, given sufficient sensitivity the microwave band offers a *unique* window on numerous vital physical processes including, but not limited to, the formation of stars in both the high and low mass regimes, as well as the earliest stages of planet formation from circumstellar disks. These processes are particularly well probed at centimetre-wavelengths as it is here that opacity effects in the hot ionized plasma around young stars are most informative and here that opacity effects in dust populations are most reduced. This historical observational bias against microwave wavelengths may also be the cause of the late discovery of the anomalous microwave emission largely attributed to spinning dust.

The AMI telescope provides a highly effective instrument for Galactic science at centimetre wavelengths, not only for its high sensitivity in the microwave band, but also for its extensive spatial dynamic range. Galactic emission exists on a broad range of scales with physical processes often strongly linked across that range. With high sensitivity and resolution from 0.5-10 arcmin AMI is ideal for probing Galactic processes on multiple scales *simultaneously*. A range of successful galactic science programmes have already been carried out by AMI. Here we review the major components of this science programme with an emphasis on where the future direction of the AMI telescope may take us in these areas.

B. Spinning Dust

1. Scientific Motivation

Anomalous Microwave Emission (AME) was termed by Leitch et al. [70] who detected dust-correlated emission at 15 GHz that could not be explained by traditional emission mechanisms (e.g. CMB, free-free, synchrotron, thermal dust). It was also easily detected by the COBE-DMR satellite [62] but was initially thought to be due to free-free emission from warm ionized gas. Since then, numerous experiments have measured AME across the sky over the frequency range 8–100 GHz (see Planck Collaboration: Ade et al. [80] and references therein). There has been much debate about the exact nature of the AME. A number of mechanisms have been proposed including hot free-free emission, hard synchrotron radiation, two-level system dust and magneto-dipole radiation (see e.g. Bennett et al. [33] for a discussion). However, the leading theory for AME is electric dipole radiation from small rapidly spinning dust grains. It has been known for a long time [47] that residual electric dipole moments of small dust grains could potentially emit detectable radio emission. However, it took 50 years for it to be detected because it appears to emit strongly in a relatively narrow range of frequencies (10-60 GHz). The theory is now relatively well understood [43, 44] although the exact details of excitation and damping of the dust grains are complicated. Statistically, on large scales ($\sim$ 1 degree) the latest results from *Planck* now appear to show definitively that spinning dust emission is indeed responsible, at least for some lines-of-sight [80]. The study of AME is now a significant area of astronomical research. Not only is it a strong foreground that must be accurately removed when measuring CMB anisotropies, particularly at frequencies near and just below the foreground minimum at $\simeq$70 GHz ([41]), and consequently understanding the spectrum of AME and mapping its morphology across the sky will aid component separation, leading to more precise measurements of the CMB; but moreover, spinning dust offers a new window into the physics of dust grains and their environs with particular emphasis on the small grain population which is crucial for controlling the physical

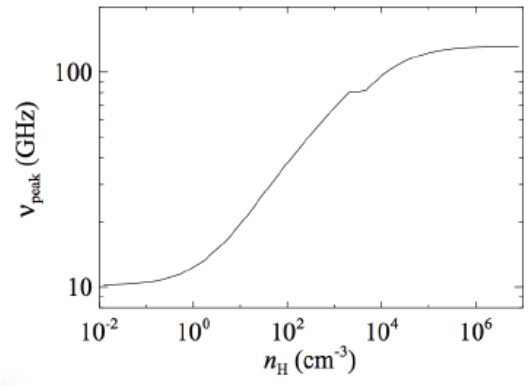

FIG. 5: Variation of the peak of the spinning dust spectrum as a function of density [2]. Lower density environments peak at < 20 GHz and are accessible to AMI.

conditions and chemistry of star forming regions. Measuring its spectrum and spatial morphology on smaller scales provides a new way to study dust that is complementary to traditional methods that typically use infrared continuum and spectroscopy.

2. Contribution of AMI

AME has been observed across the sky by numerous experiments. However, the majority of these have been CMB experiments that work at higher frequencies (> 20 GHz) and at relatively low angular resolution (5 arcmin). On large angular scales the most important dataset has been from the WMAP satellite, due to its lowest two frequency channels at 23 GHz and 33 GHz. New data from the *Planck* satellite is already producing astonishing new results but the data are limited to its lowest frequency channel at 30 GHz with 30 arcmin resolution. With satellites such as WMAP and *Planck* limited to large angular scales and high frequencies, it is therefore crucial to survey the sky at higher angular resolution and at frequencies below those accessible to *WMAP* and *Planck* to gain a complete understanding of this emission. The AMI instrument is therefore perfectly matched for studying AME for multiple reasons: its frequency range (12-18 GHz) covers the low side and peak of spinning dust emission; its high angular resolution (2 arcmin for AMI-SA) allows it to be well-matched to radio surveys at lower frequencies and to localise emission, whilst the size of its primary beam (20 arcmin) is well matched to CMB experiments at higher frequencies, including *Planck*; the compact nature of the array results in high surface brightness sensitivity and consequently high spatial dynamic range mapping; when combined with the Large Array it is able to investigate and separate the source population with high precision, which is especially valuable in star forming regions.

These benefits have been demonstrated to good effect by the significant contribution to spinning dust research that AMI has already made [13–17]. In addition a recent survey of the Perseus molecular cloud region is showing spectacular results. The detailed structure and comparison with infrared tells us that the spinning dust critically depends on location and environment [2]. More observations of diffuse clouds are needed to unravel this complicated picture and relate it to theoretical predictions and AMI is ideally suited to these kinds of surveys. In addition, *Planck* is already detecting new AME candidates that will need follow-up at high resolutions. AMI data can confirm whether the AME is indeed diffuse emission or if the large *Planck* beam is contaminated by compact HII regions that are emitting optically thick emission at high (> 10 GHz) frequencies. The frequency coverage of AMI can pin down the peak of the spinning dust spectrum, which in the most diffuse regions appears to be below 20 GHz. In the more dense regions, AMI can measure the rise at low frequencies due to the larger grains and the data are complementary to that at higher frequencies. Fig. 5 shows how the peak of the spinning dust curve, which can be as low as 10 GHz, varies with density. Although other arrays can probe this frequency range (e.g. JVLA, ATCA), they do not have the brightness sensitivity required to measure diffuse emission on arcminute scales.

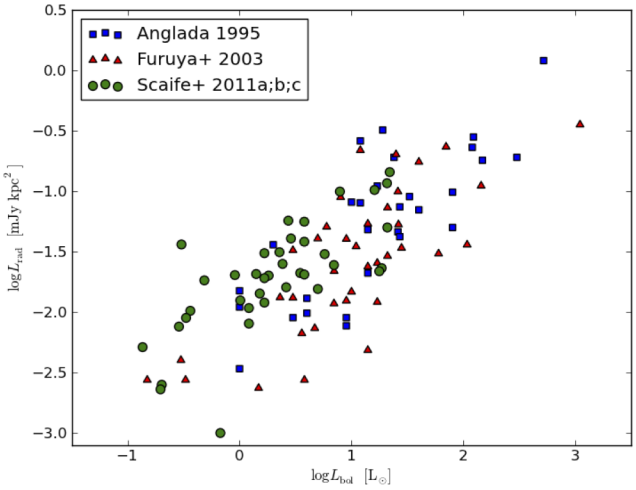

FIG. 6: Correlation of radio luminosity with bolometric luminosity for Class 0 & I YSOs

C. Low Mass Star Formation

1. *Scientific Motivation*

Since the advent of the *Spitzer* space telescope, direct infrared detection of the hot dust heated by an embedded protostar has become the most popular method for differentiating between starless and protostellar cores. Although the method is extremely reliable, *Spitzer* identification is not completely certain [58] as the response to extragalactic radio sources is known to mimic that of embedded protostellar cores and can cause false detections. In addition, a protostellar spectrum alone will not demonstrate that a core is truly embedded and, like many surveys, *Spitzer* is also flux-limited, with a luminosity completeness limit of $0.004(d/140\ \mathrm{pc})^2\ L_\odot$ [45, 57]. Correctly determining the relative numbers of starless and protostellar cores in star-forming regions is essential for inferring timescales for the different stages of protostellar evolution; for low-luminosity objects it is also necessary to determine the extent of the luminosity problem first articulated by Kenyon & Hartmann [60] in order to understand the accretion mechanisms underlying protostellar evolution.

Identifying embedded protostars by detecting their molecular outflows, either via high-excitation jet interactions (Herbig-Haro objects and shock-excited H_2; e.g. Davis et al. [42], Walawender, Bally, & Reipurth [90]) or through low-excitation molecular lines such as ^{12}CO, can immediately identify a source as an embedded protostar, avoiding the contaminants of infrared colour selection. However, in crowded star-formation regions, confusion from neighbouring outflows can frequently be an issue. Radio emission (see e.g. Andre, Ward-Thompson & Barsony [25]) is a reliable method for detecting protostars, as well as providing a potential mechanism for distinguishing protostellar class via its correlations with other physical characteristics.

2. *Contribution of AMI*

Radio follow-up of the Dunham et al. [45] *Spitzer* catalogue of low luminosity embedded objects at 15.7 GHz [18–20] (see Fig. 6) has provided clear evidence for distinct trends in the behaviour of the radio luminosity of these sources when compared with their bolometric luminosity, IR luminosity and outflow force where molecular outflows have been measured. Similar trends are well-documented at lower radio frequencies for higher luminosity sources ($< 10^3\,\mathrm{L}_\odot$; see e.g. Anglada et al. [27] or Shirley et al. [86]). In addition, the relationship between radio luminosity and the IR luminosity of these objects has shown that it may be possible to use the radio emission as a proxy for the internal luminosity of low luminosity objects, a quantity which can otherwise only be derived through complex modelling of the IR spectra. The cm emission probes the current mass ejection directly, without the historical averaging inherent in CO outflows, and originates from the inner protostellar core which will be the subject of ALMA and EVLA studies. The cm datapoints on the SED provide constraints both on the free-free emission geometry and on the relative contributions of thermal dust and bremsstrahlung [4].

Blind surveys for radio protostars will be intrinsically biased towards young objects [20] and the radio emission from heavily embedded sources may provide an excellent method for confirming the Class 0 population. This is of particular importance in light of the newly discovered VeLLO objects, many of which are still heavily embedded. Such objects are difficult to confirm in the infra-red [37] or through molecular mapping [38, 40], but nevertheless represent an important population for theories of non-steady accretion. AMI provides an important resource for studies to confirm and characterize low luminosity sources. As has already been demonstrated by the instrument, the cm-wave band is an excellent probe of protostellar activity. Blind surveys of molecular clouds with the AMI-LA that are currently in progress will also provide key information on young embedded objects which may previously have been missed by surveys at higher frequencies.

D. High Mass Star Formation

1. Scientific Motivation

In recent years we have started to realise that the early lives of young HII regions (the ultracompact & hypercompact phases) may be dynamic epochs in the star formation process, with complex accretion flows through the ionisation boundary [54] that are often mediated by Rayleigh-Taylor instabilities [67]. The classical picture of young HII regions is one of simple pressure-driven expansion whereby the central star has finished accretion, has reached the main sequence, and the surrounding HII region is expanding at the sound speed into the surrounding ISM. However, recent observations of ultracompact and hypercompact HII regions reveal that often infall and accretion are ongoing in both the surrounding molecular (e.g. Beltrán et al. [31], Klaassen et al. [61]) and ionised gas [32, 53] and more intriguingly, some ultracompact and hypercompact regions show evidence of variability on timescales of a year [1, 51, 53].

Detailed modelling of HII region variability has been carried out by Galván-Madrid et al. [54], Peters et al. [78], who find that the radio flux of young HII regions changes in direct response to sudden increases in the accretion of material onto the star. As the accretion rate increases the HII region reduces in size and is quenched. Thus tracking the time-variable radio flux from the ultra and hypercompact HII regions in the Peters et al. model enables the accretion rate onto the star to be inferred, and offers the unique prospect of determining the accretion history. By comparison, to determine the accretion history via spectroscopic measurements of the small-scale velocity structure (a few hundred AU) around the star would require angular resolution better than ∼10 milli-arcsec — a challenging target for interferometers. Determining the accretion history for massive star formation will allow current star formation models (e.g. Bonnell et al. [35], McKee & Tan [75]) to be confronted directly.

2. Contribution of AMI

AMI is of fundamental value in this kind of study. Firstly, the operating frequency of 15.7 GHz is close to the peak in the spectrum of most ultracompact HII regions and takes full advantage of the steep positive spectral index of hypercompact HII regions (e.g. Kurtz [68]). This is shown in Figure 7, which shows the SED of ultracompact, hypercompact and classical HII regions. Secondly, AMI is an excellent telescope for carrying out variability studies as the system and calibration are both stable and well-understood. Finally, AMI has sufficient flexibility in its schedule to enable variability studies with a range of cadences. It will be important to identify isolated ultracompact and hypercompact regions for variability studies with AMI, due to the $30''$ beam of the Large Array and the typical clustering of massive star forming regions. Such isolated sources can be identified from the northern section of the CORNISH survey (for ultracompact HII regions only, Purcell & Hoare [84]), the Torun and MMB methanol maser surveys (by searching for associated hypercompact HII regions, e.g. Longmore et al. [71]), and the *Herschel* Hi-GAL survey [77]. Conducting an AMI variability study on isolated young HII regions in the North will not only give us a greater understanding of the accretion processes involved in massive star formation, but will also feed into the much larger statistical studies possible at sub-arcsecond resolution with MeerGAL, the MeerKAT 14 GHz Galactic Plane Survey.

The high sensitivity of the AMI-LA has already been demonstrated as providing an excellent tool for long term monitoring programmes of HCHII regions (AMI Consortium: Scaife et al., in prep.) using total flux density as a tracer of expansion and contraction for optically thick emission. In addition the AMI Galactic Plane Survey will provide a unique resource in the Northern hemisphere for detecting new HCHII regions due to its large area coverage (860 square degrees) and depth (AMI Consortium: Perrott et al., in prep.).

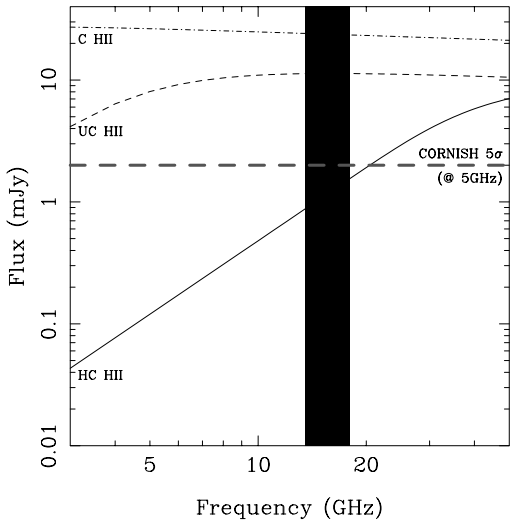

FIG. 7: Theoretical spectra of isothermal young homogeneous HII regions at a distance of 20 kpc. Solid, dashed and dot-dashed lines show spectra for hypercompact, ultracompact and compact HII regions respectively, with typical emission measures taken from Kurtz [68]. We show the 5GHz 5σ flux limit for the CORNISH survey by a horizontal line, and the frequency range of AMI with a solid vertical bar. Operating at 15.7 GHz will enable us to study ultracompact, hypercompact and compact HII regions.

E. Planet Formation

1. Scientific Motivation

The growth of dust grains from sub-micron to micron sizes in the local environment of protostellar objects is well-probed by observational data in the mid-infrared; however, the further growth of these grains to larger sizes is only probed by their sub-mm and cm-wave emission. It is this growth, and the possible coagulation and sedimentation that follows it, which is widely thought to lead to the formation of proto-planetary objects in the dense disks around evolving protostars. Measuring the long wavelength tail of the thermal emission from dust, which is expected to be dominated by such large dust grains, often referred to as pebbles, provides an independent measure of the dust composition in the disk through its opacity index (β), as well as the mass of the accumulated matter in the disk which is an important factor in models of planet formation (e.g. Boss [36]).

Sub-mm measurements towards circumstellar disks are often used to determine the mass of proto-planetary disks and hence their potential for planet formation. Alternative methods of disk mass estimation, such as spectral line measurements of molecular gas, are complicated by opacity effects (e.g. Beckwith & Sargent [30]) and require complex models to account for these effects as well as those of depletion [46, 59]. Sub-mm and radio measurements are useful not only as a probe of the disk mass itself, but, with multi-wavelength data available, they can also be used to determine the evolution of the opacity index as a function of frequency [87, 88] and place constraints on the growth of dust grains in such disks. This in turn will show whether the timescales assumed in current models of planet formation are consistent with observational data. However, comparison of disk evolution models and sub-mm data indicate that in 10^5 yrs dust grains will have already grown to a size large enough to cause substantial opacity effects and hence problems in estimating disk masses on the basis of sub-mm data alone. Consequently, it is likely that sub-mm data can only provide reliable disk masses for Class 0 objects. These values are subject to caveats in the context of further planet formation as at this evolutionary stage there is also expected to be significant accretion from the disk onto the central object [56]. Indeed, to date the disk masses determined from sub-mm data appear to be too low to agree with theoretical models of planet formation (see e.g. Andrews & Williams [26]).

2. Contribution of AMI

At the resolution of the AMI-LA ($\simeq 25$ arcsec) it is not possible to resolve the structure of proto-planetary disks. However, at cm-wave frequencies the contribution from the larger dust envelope around proto-planetary systems has a

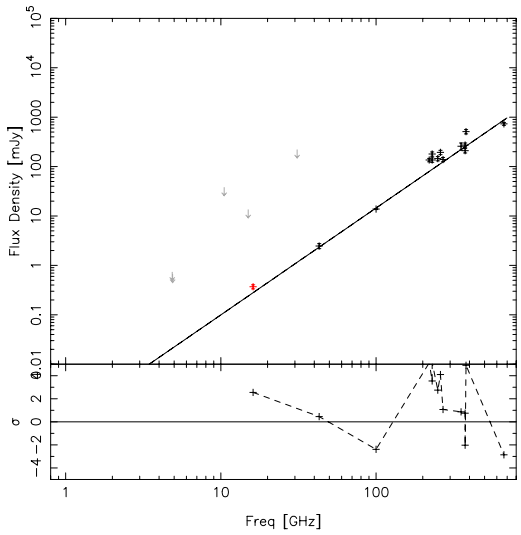

FIG. 8: SED of DO Tau (Class II). Black data points are taken from the literature, red data point from the AMI-LA, and grey arrows indicate upper limits from the literature (AMI Consortium: Scaife et al., in prep.).

negligible contribution to the flux density (typically $< 1\,\mu$Jy) for the Class I objects where planet formation is thought to initiate; consequently the need for high resolution to separate the disk and envelope contributions, which arises at sub-mm wavelengths, is not as pressing. At the observing wavelength of AMI $\lambda \simeq 2\,$cm it is also the case that the disk emission will be optically thin in the vast majority of cases, negating the optical depth considerations which affect the disk mass estimates made at higher frequencies. Consequently using cm-wave data to estimate disk masses provides a method which is far more applicable for the more evolved Class I & II objects where planet formation is starting to occur. This has already been demonstrated as a proof of concept with AMI using a sample of disks in the Taurus molecular cloud [21] where cm-wave disk masses were found to be systematically higher than those derived from sub-mm data, boosting them above the minimum-mass threshold required for giant planet formation. Future work with AMI in this area has the potential to better constrain not only theories of planet formation through disk mass evaluation, but also, through placing limits on the opacity index of the disk material, the evolution of the grain growth within such disks, see Fig 8. These data are very different from and highly complementary to those from the JVLA, as well as the ALMA telescope, particularly the proposed Band 1 instrument at 30 GHz.

IV. TRANSIENT AND VARIABLE-SOURCE ASTROPHYSICS

A. Introduction

AMI-LA, mainly in its former guise as the Ryle Telescope (RT), has been an extremely successful telescope in providing key radio monitoring and follow-up data on a number of high-energy astrophysical sources, e.g. X-ray binaries (XRBs) and gamma-ray bursts (GRBs). This has been an extremely productive area in terms of publications and citations (for example, there are over 3000 citations for papers by Fender and/or Pooley from this).

In the following, we provide examples of some of the key results over this period, and then discuss what AMI can do in this area in the future.

B. Key AMI-LA / RT Results on Transients

The AMI-LA has been used extensively to monitor currently active XRBs, systems that contain an accreting neutron star (NS) or black hole (BH). These systems are the sites of some of the most extreme astrophysics in the Universe, and black-hole accretion has been shown to be mass-scalable such that we can learn about AGN accretion

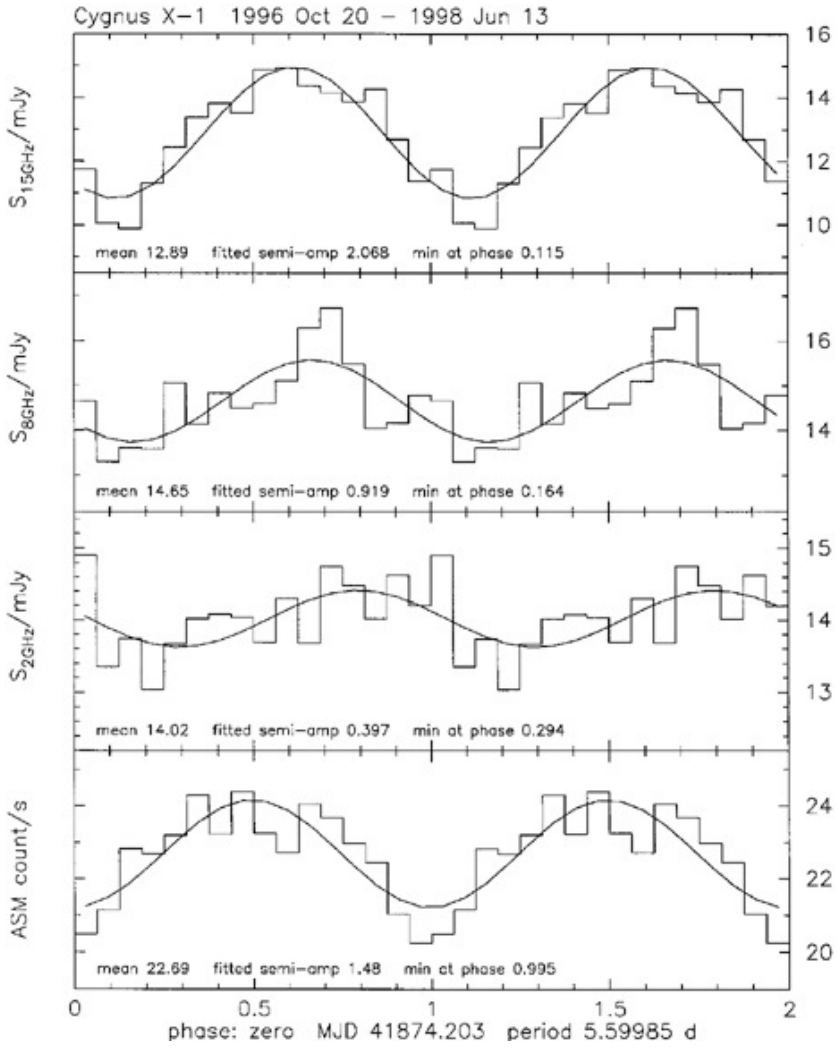

FIG. 9: Orbital modulation of the 15.7-GHz radio emission from the black-hole binary Cygnus X-1. From Pooley, Fender, & Brocksopp [83].

and feedback from studying BH XRBs (and vice versa).

A handful of systems are 'persistently active', including several famous XRBs such as Cygnus X-1, Cygnus X-3, GRS 1915+105 and SS433. The AMI-LA datasets on these objects, in particular the first three, are simply the most comprehensive datasets in existence on the variability of relativistic jets (which produce the radio emission) and their connection to the accretion flow (as observed in X-ray and infrared).

In addition, there are a large number of transient systems, notably XRBs in outburst, and GRB afterglows, which show transient radio emission for a period of typically a few months.

1. Cygnus X-1

Cygnus X-1 is the archetypal 'black-hole candidate', and contains a $\simeq 10\,M_\odot$ BH in orbit around an OB-type companion star. The source accretes persistently around $\simeq 2\%$ of its Eddington luminosity, nevertheless undergoing accretion state changes, as revealed by occasional strong changes in the X-ray spectral and timing behaviour (see Figure 9).

The AMI-LA monitoring of Cygnus X-1 has provided a key data set for understanding the jet in this system, which has been demonstrated to be rather powerful in the long term [52] and *possibly* associated with a the black hole which is possibly rapidly spinning [55].

One of several key discoveries of the AMI-LA for Cygnus X-1 is that the radio emission is modulated at the 5.6-day orbital period [83]. This is a unique situation in the whole of astrophysics: the regular passage of the inner regions of a relativistic jet moving through the dense parts of the OB star stellar wind provide variable free-free absorption along the line of sight. These data provide rich constraints on the location and size of the relativistic jet (see e.g. Zdziarski et al. [93]).

2. Cygnus X-3

Just as for Cygnus X-1, the Cygnus X-3 data taken by the AMI-LA and RT over more than 30 years of monitoring are a unique resource for understanding jets. The data have generated many tens of papers.

A key recent result, however, was that the high-energy gamma-ray emission from Cygnus X-3, as measured with *Fermi*, was found to be correlated with periods of radio flaring (observed with AMI-LA, see Figure 10). This clearly established a direct link between the presence of strong jet activity and the production of high energy gamma-rays [49].

3. GRS 1915+105

In 1992, a new bright BH XRB, GRS 1915+105, was discovered. This source became famous as the first source of apparently superluminal jets in the Galaxy [76], and has remained active at close to its Eddington luminosity ever since.

The X-ray behaviour of GRS 1915+105 is extraordinary. The source switches rapidly between three different X-ray 'states', associated with which are clearly correlated changes in the radio emission, indicating that the jet can be launched, vary, and be shut off all on timescales of minutes. The vast array of simultaneous X-ray, infrared and radio observations of GRS 1915+105 are the most important single resource, *in the whole of astrophysics*, for understanding the connection between accretion and outflow.

Careful study of these data led, eventually, to the unified empirical model for the connection between accretion and jets in black holes published in Fender, Belloni, & Gallo [48] (see Figure 11). This model remains consistent with all data to the present day, and appears to be applicable in large part to supermassive accreting black holes in AGN Körding, Jester, & Fender [64].

4. Tidal-Disruption Event

Many transient events, mostly X-ray binaries, SNe, AGN or GRB, have been observed with the AMI-LA (and its predecessors). The source *Swift* J164449.3+573451, initially thought to be a GRB, is now believed to be an exceptionally unusual tidal-disruption event: a star that has been captured by an otherwise quiescent BH in a galactic nucleus. The radio emission at 15.7 GHz has peaked after some 130 days, and is now declining gently. It should be visible for some years, and may well be resolvable by VLBI instruments in due course. There is a wide range of astrophysical information to be extracted from the current set of observations, of which the AMI-LA is one of the best sampled.

C. Contribution of AMI in The Future

AMI has demonstrated itself to be an extremely efficient, effective and important radio telescope for the follow-up and monitoring of high-energy astrophysical transients. This is for a number of reasons, which include:

1. **Highly-flexible scheduling** — possibility of both rapid response and regular monitoring.
2. **High radio frequency** — astrophysical events vary more rapidly, and more in tune with other wavelengths, at higher radio frequencies. This is because the lower optical depth probes closer to the jet 'launch site'. The insights we made into the disk-jet coupling in GRS 1915+105 and other sources would simply not have been possible at, say, 1 GHz, where the variations are 'blurred' out in time and width from the launch event. At 15.7 GHz there is also much less confusion and long runs are not required to measure 'core' radio-flux densities.

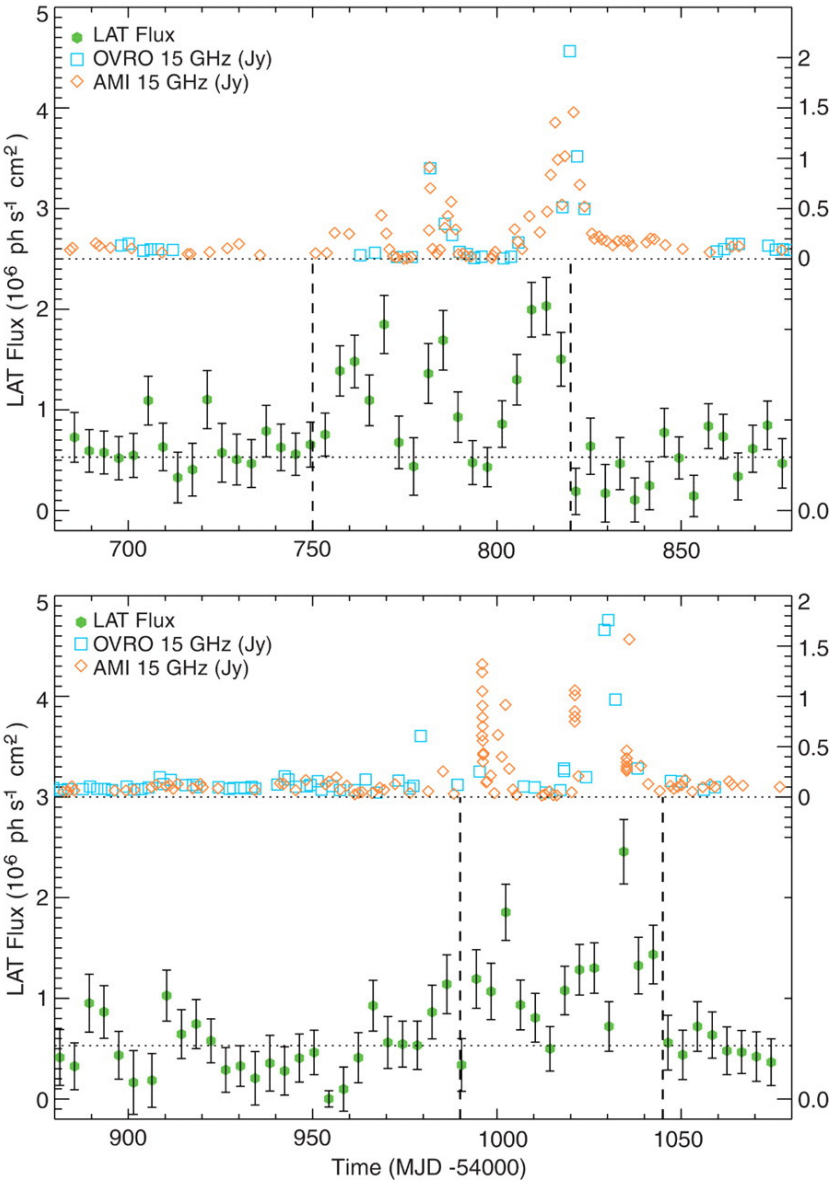

FIG. 10: Detection of gamma-ray emission coincident with periods of radio flaring in the XRB Cygnus X-3. From Fermi LAT Collaboration et al. [49].

Future operations of AMI will exploit and develop this capability.

Regarding (1), Cambridge and Southampton Universities have recently developed software for the automatic triggering of an AMI override observation based upon a VO Event alert (see e.g. skyalert.org and Section V A). This system has been used for 'target-of-opportunity' observations towards M31 ULX-1, GRB120305A, GRB120308A and GRB120311A. In parallel, development has begun on software to automatically parse VO Events (xml format), make evaluations and decisions and ultimately in some cases trigger an observation. This work is part of a broader effort towards coordinated and intelligent transient observations which includes teams from LOFAR, MeerKAT, the EVN and the VO. Since AMI's scheduled observations involve comparatively long, repeated measurements, such 'targets of opportunity' can generally be observed *promptly*, with little impact on existing programmes.

Regarding (2), although there will in some cases be merit in triggering AMI based upon LOFAR, in most cases the exciting astrophysical event will have happened significantly earlier than the point at which the MHz radio emission peaks (specifically this is true for synchrotron emission; some events may have very early coherent bursts). The delay between emission peaks at GHz and MHz frequencies can be weeks for XRBs, and years for GRB afterglows. Triggering on *radio* (as opposed to e.g. X-ray or gamma-ray) transients should therefore be based on detections at as

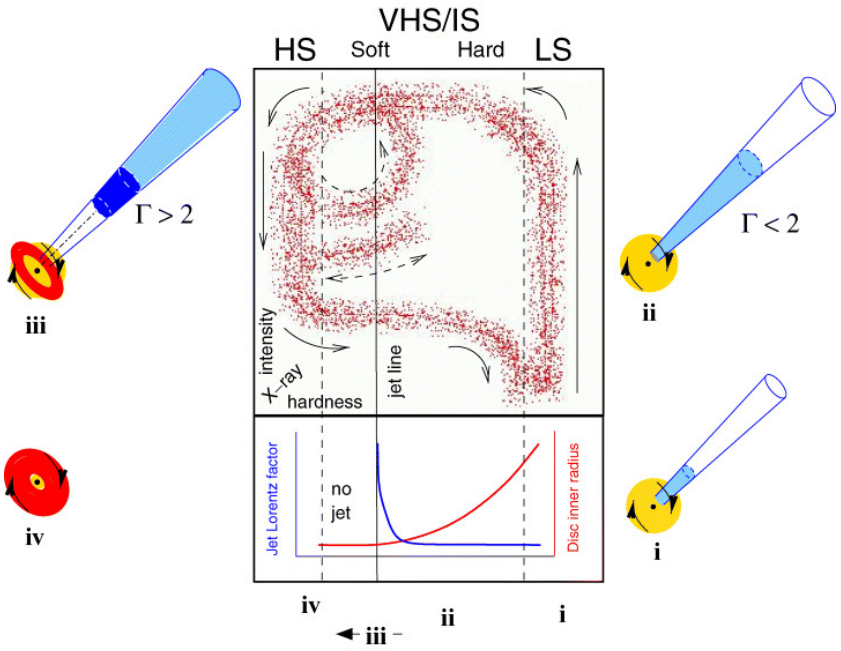

FIG. 11: The unified empirical model for the coupling between accretion and jet formation in BH XRBs from Fender, Belloni, & Gallo [48]. The model has been tested extensively and seems to hold, and to also be applicable to AGN. Development of the model was led in large part by the vast AMI-LA database on the highly-variable BH GRS 1915+105.

high a radio frequency as possible. In this case APERTIF, the focal plane array upgrade to WSRT, which will provide a ~ 3 deg^2 field of view in the 1-GHz band, will probably be superior to LOFAR for providing transient detections that are scientifically complemented by AMI data. APERTIF has several proposed key science projects in the area of transients (to be evaluated in 2012). Furthermore there is overlap of the sky visible to AMI with MeerKAT and ASKAP, and the test arrays KAT-7 and BETA. Both SKA precursors have embraced transient detection with both image-plane and time-series approaches approved and under development. Interestingly, the survey figures of merit for ASKAP, APERTIF, MeerKAT and also the JVLA are all comparable, indicating similar potential GHz transient yields (depending on observing strategy) over the coming decade. Unlike gamma-ray and X-ray transients (with some exceptions, notably those found by *Swift*), which are typically localised (initially) only to a few degrees (and therefore unsuitable for a simple rapid AMI follow-up without more complex tiling), these radio transients will be localised with $\simeq$arcsec accuracy.

V. UPGRADES TO AMI

A. Automatic Target-of-Opportunity Facility

At the beginning of 2012, a collaboration between Southampton and Cambridge Universities developed a fully automated rapid follow-up facility for observation of transient events. As a first implementation of this new "robotic facility" we have focused on follow-up of the well localised GRB events observed by the *Swift* burst-alert telescope Barthelmy et al. [29]. Staley et al. 2012 (in prep) will describe the AMI observations of the first ten *Swift* GRB targets, seven of which were initiated within minutes of the GRB alert being distributed via the NASA GCN network. This automatic target-of-opportunity (ToO) facility comprises three subsystems:

- The distribution network, making use of the VOEvent standard [91] implemented through a Python software package ('Comet'; https://github.com/jdswinbank/Comet). We monitor new GRB events detected by the *Swift* burst alert telescope, via a direct connection to the recently announced GCN VOEvents service. This approach can be easily extended as more sources of transient event data become available.

- The observation request trigger, which uses a simple filter to extract the required information and then generates a specially formatted observation request email which is sent to the AMI control computers.

- The automated telescope response, which is implemented through an in-house program, RQCHECK that validates the email, checks syntax and keyword values, and then:
  - Checks if target is currently on-sky and is unobscured by the Sun or Moon.
  - Determines the observation time according to the timing specified in the request (ASAP, next transit, or specified sidereal time).
  - Finds the nearest phase calibrator from VLBA and JVAS catalogues.
  - Checks the availability of the telescope, e.g. in case of priority observing or engineering work.
  - Constructs an entry for the observing queue.
  - Inserts this entry in the queue, rescheduling other entries.
  - Notifies the requester of the outcome by e-mail.

Our current trigger policy is to issue an observation request to AMI-LA for all *Swift* GRB alerts with a declination above -10°. We follow up GRBs which are detected during the ToO observation with an ad-hoc schedule determined individually for each source. For radio non-detections we employ a logarithmic follow-up schedule with additional observations after 1-2 days, 3-4 days, 1 week, 2 weeks, and finally at 1 month.

B. Digital Correlator Upgrade

The current AMI correlator is an analogue lag, Fourier-transform spectrometer, which synthesises eight 0.75-GHz channels from sixteen sampled measurements of the real part of each baseline's correlation at 25mm delays. The 0.75-GHz wide channels are narrow enough to prevent bandwidth smearing, but we find that they provide insufficient spectral rejection to remove the effects of transmissions from geostationary satellites, even with hardware filters in both the RF and IF chains. At present, transmissions from geostationary satellites hamper AMI observations at declinations below 20 degrees: at dec 15 degrees, about ten percent of time-domain data have to be excised, and by 0 degrees 95 percent of data are corrupted. This is a major problem because the equatorial sky is accessible to both northern and southern telescopes and, by the same token, deep legacy fields in many wavebands are equatorial. A digital correlator would offer many more, much narrower channels over the observing band, and spectral filtering would becomes feasible, improving the situation dramatically. The technology of analogue-to-digital converters (ADCs) has rapidly advanced to the extent that 4-bit, 10 giga-sample per second ADCs are available at modest cost, making an affordable digital correlator for AMI a possibility. As part of a successful ERC Starting Grant application, Scaife (Southampton) has secured full funding to allow the construction of a new digital correlator and this upgrade to AMI will give AMI exciting new capabilities:

- Most importantly AMI will be able to image equatorial regions of the sky which are currently inaccessible. This will allow many new science programmes with observations towards key extragalactic deep fields (e.g. COSMOS, Subaru/XMM-Newton Deep Survey UKIDSS-Ultra-Deep Survey, VIDEO) and AMI will be able to image sky visible to both ALMA and VISTA.
- Spectral filtering of the visibilities will reduce the fraction of data excised for RFI, increasing the frequency lever-arm for spectral work such as AME and increasing the overall sensitivity.
- The new correlator will not suffer from systematics associated with lag spacing errors in the Fourier-transform spectrometer, and this will increase the imaging dynamic range, allowing robust removal of much brighter contaminating radio sources in SZ fields.
- The increased spectral resolution of the correlator will allow for better identification of contamination and so reduce systematics in the final images.

VI. FUTURE OPERATIONAL MODEL

Until now the scientific direction for AMI has been determined by the Cavendish Astrophysics Group in Cambridge, although a great many external collaborations have been formed and have yielded the broad variety of science described above. The aim now is to change the operational model for AMI, opening up the telescope to external observers, to maximise new scientific return. A consortium of UK universities will bid to the STFC for operations funding and will determine the scientific programme for AMI, inviting observing proposals from the community. This will allow new programmes to be initiated to exploit the unique capabilities for low-surface-brightness, centimetre-wavelength observation offered by AMI.

VII. REFERENCES

[1] Acord J. M., Churchwell E., Wood D. O. S., 1998, ApJ, 495, L107
[2] Ali-Haïmoud Y., Hirata C. M., Dickinson C., 2009, MNRAS, 395, 1055
[3] Allen S. W., Evrard A. E., Mantz A. B., 2011, ARA&A, 49, 409
[4] AMI Consortium: Ainsworth R. E., et al., 2012, MNRAS, 423, 1089
[5] AMI Consortium: Barker R. et al., 2006, MNRAS, 369, L1
[6] AMI Consortium: Davies M. et al., 2011, MNRAS, 415, 2708
[7] AMI Consortium: Franzen T. et al., 2011, MNRAS, 415, 2699
[8] AMI Consortium: Hurley-Walker N., et al., 2011, MNRAS, 414, L75
[9] AMI Consortium: Hurley-Walker N. et al., 2012, MNRAS, 419, 2921
[10] AMI Consortium: Olamaie M. et al., 2012, MNRAS, 421, 1136
[11] AMI Consortium: Rodríguez-Gonzálvez C. et al., 2011, MNRAS, 414, 3751
[12] AMI Consortium: Rodríguez-Gonzálvez C. et al., 2012, MNRAS, 3459
[13] AMI Consortium: Scaife A. M. M., et al., 2008, MNRAS, 385, 809
[14] AMI Consortium: Scaife A. M. M., et al., 2009, MNRAS, 394, L46
[15] AMI Consortium: Scaife A. M. M., et al., 2009, MNRAS, 400, 1394
[16] AMI Consortium: Scaife A. M. M., et al., 2010, MNRAS, 403, L46
[17] AMI Consortium: Scaife A. M. M., et al., 2010, MNRAS, 406, L45
[18] AMI Consortium: Scaife A. M. M., et al., 2011, MNRAS, 410, 2662
[19] AMI Consortium: Scaife A. M. M., et al., 2011, MNRAS, 415, 893
[20] AMI Consortium: Scaife A. M. M., et al., 2012, MNRAS, 420, 1019
[21] AMI Consortium: Scaife A. M. M., et al., 2011, arXiv, arXiv:1111.5184
[22] AMI Consortium: Shimwell T., et al., 2012, 2012, MNRAS, 423, 1463
[23] AMI Consortium: Zwart J. T. L., et al., 2008, MNRAS, 391, 1545
[24] AMI Consortium: Zwart J. T. L., et al., 2011, MNRAS, 418, 2754
[25] Andre P., Ward-Thompson D., Barsony M., 1993, ApJ, 406, 122
[26] Andrews S. M., Williams J. P., 2005, ApJ, 631, 1134
[27] Anglada G., Estalella R., Mauersberger R., Torrelles J. M., Rodriguez L. F., Canto J., Ho P. T. P., D'Alessio P., 1995, ApJ, 443, 682
[28] Arnaud M., Pratt G. W., Piffaretti R., Böhringer H., Croston J. H., Pointecouteau E., 2010, A&A, 517, A92
[29] Barthelmy S. D., et al., 2005, SSRv, 120, 143
[30] Beckwith S. V. W., Sargent A. I., 1993, ApJ, 402, 280
[31] Beltrán M. T., Cesaroni R., Zhang Q., Galván-Madrid R., Beuther H., Fallscheer C., Neri R., Codella C., 2011, A&A, 532, A91
[32] Beltrán M. T., Cesaroni R., Codella C., Testi L., Furuya R. S., Olmi L., 2006, Natur, 443, 427
[33] Bennett C. L., et al., 2003, ApJS, 148, 97
[34] Berger E., Zauderer A., Pooley G. G., Soderberg A. M., Sari R., Brunthaler A., Bietenholz M. F., 2012, ApJ, 748, 36
[35] Bonnell I. A., Smith R. J., Clark P. C., Bate M. R., 2011, MNRAS, 410, 2339
[36] Boss A. P., 1998, ApJ, 503, 923
[37] Bourke T. L., et al., 2006, ApJ, 649, L37
[38] Bourke T. L., Crapsi A., Myers P. C., Evans N. J., II, Wilner D. J., Huard T. L., Jørgensen J. K., Young C. H., 2005, ApJ, 633, L129
[39] Clowe D., Bradač M., Gonzalez A. H., Markevitch M., Randall S. W., Jones C., Zaritsky D., 2006, ApJ, 648, L109
[40] Crapsi A., et al., 2005, A&A, 439, 1023
[41] Davies R. D., 2006, cmb..conf,
[42] Davis C. J., Scholz P., Lucas P., Smith M. D., Adamson A., 2008, MNRAS, 387, 954
[43] Draine B. T., Lazarian A., 1998, ApJ, 494, L19
[44] Draine B. T., Lazarian A., 1998, ApJ, 508, 157
[45] Dunham M. M., Crapsi A., Evans N. J., II, Bourke T. L., Huard T. L., Myers P. C., Kauffmann J., 2008, ApJS, 179, 249
[46] Dutrey A., Guilloteau S., Simon M., 2003, A&A, 402, 1003
[47] Erickson W. C., 1957, ApJ, 126, 480
[48] Fender R. P., Belloni T. M., Gallo E., 2004, MNRAS, 355, 1105
[49] Fermi LAT Collaboration, et al., 2009, Sci, 326, 1512
[50] Feroz F., Hobson M. P., Zwart J. T. L., Saunders R. D. E., Grainge K. J. B., 2009, MNRAS, 398, 2049
[51] Franco-Hernández R., Rodríguez L. F., 2004, ApJ, 604, L105
[52] Gallo E., Fender R., Kaiser C., Russell D., Morganti R., Oosterloo T., Heinz S., 2005, Natur, 436, 819
[53] Galván-Madrid R., Keto E., Zhang Q., Kurtz S., Rodríguez L. F., Ho P. T. P., 2009, ApJ, 706, 1036
[54] Galván-Madrid R., Peters T., Keto E. R., Mac Low M.-M., Banerjee R., Klessen R. S., 2011, MNRAS, 416, 1033

[55] Gou L., et al., 2011, ApJ, 742, 85
[56] Greaves J. S., Rice W. K. M., 2011, MNRAS, 412, L88
[57] Harvey P., Merín B., Huard T. L., Rebull L. M., Chapman N., Evans N. J., II, Myers P. C., 2007, ApJ, 663, 1149
[58] Hatchell J., Dunham M. M., 2009, A&A, 502, 139
[59] Kamp I., Dullemond C. P., 2004, ApJ, 615, 991
[60] Kenyon S. J., Hartmann L. W., 1990, ApJ, 349, 197
[61] Klaassen P. D., Wilson C. D., Keto E. R., Zhang Q., 2009, ApJ, 703, 1308
[62] Kogut A., Banday A. J., Bennett C. L., Gorski K. M., Hinshaw G., Smoot G. F., Wright E. I., 1996, ApJ, 464, L5
[63] Komatsu E., et al., 2011, ApJS, 192, 18
[64] Körding E. G., Jester S., Fender R., 2006, MNRAS, 372, 1366
[65] Korngut P. M., et al., 2011, ApJ, 734, 10
[66] Kravtsov A. V., Vikhlinin A., Nagai D., 2006, ApJ, 650, 128
[67] Kuiper R., Klahr H., Beuther H., Henning T., 2011, ApJ, 732, 20
[68] Kurtz S., 2005, IAUS, 227, 111
[69] Kunz M. W., Schekochihin A. A., Cowley S. C., Binney J. J., Sanders J. S., 2011, MNRAS, 410, 2446
[70] Leitch E. M., Readhead A. C. S., Pearson T. J., Myers S. T., 1997, ApJ, 486, L23
[71] Longmore S. N., Burton M. G., Barnes P. J., Wong T., Purcell C. R., Ott J., 2007, MNRAS, 379, 535
[72] Lueker M., et al., 2010, ApJ, 719, 1045
[73] Marriage T. A., et al., 2011, ApJ, 737, 61
[74] Mason B. S., et al., 2010, ApJ, 716, 739
[75] McKee C. F., Tan J. C., 2003, ApJ, 585, 850
[76] Mirabel I. F., Rodríguez L. F., 1994, Natur, 371, 46
[77] Molinari S., et al., 2010, A&A, 518, L100
[78] Peters T., Mac Low M.-M., Banerjee R., Klessen R. S., Dullemond C. P., 2010, ApJ, 719, 831
[79] Planck Collaboration: Ade P. A. R., et al., 2011, A&A, 536, A8
[80] Planck Collaboration: Ade P. A. R., et al., 2011, A&A, 536, A20
[81] Planck Collaboration: Aghanim N., et al., 2011, A&A, 536, A10
[82] Planck Collaboration: Aghanim N., et al., 2012, arXiv:1204.1318
[83] Pooley G. G., Fender R. P., Brocksopp C., 1999, MNRAS, 302, L1
[84] Purcell C. R., Hoare M. G., 2010, HiA, 15, 781
[85] Reichardt C. L., et al., 2012, arXiv, arXiv:1203.5775
[86] Shirley Y. L., Claussen M. J., Bourke T. L., Young C. H., Blake G. A., 2007, ApJ, 667, 329
[87] Shirley Y. L., Huard T. L., Pontoppidan K. M., Wilner D. J., Stutz A. M., Bieging J. H., Evans N. J., II, 2011, ApJ, 728, 143
[88] Shirley Y. L., Mason B. S., Mangum J. G., Bolin D. E., Devlin M. J., Dicker S. R., Korngut P. M., 2011, AJ, 141, 39
[89] Sievers J. L., et al., 2009, arXiv, arXiv:0901.4540
[90] Walawender J., Bally J., Reipurth B., 2005, AJ, 129, 2308
[91] Williams R. D., Seaman R., 2006, ASPC, 351, 637
[92] Zauderer B. A., et al., 2011, Natur, 476, 425
[93] Zdziarski A. A., Skinner G. K., Pooley G. G., Lubiński P., 2011, MNRAS, 416, 1324